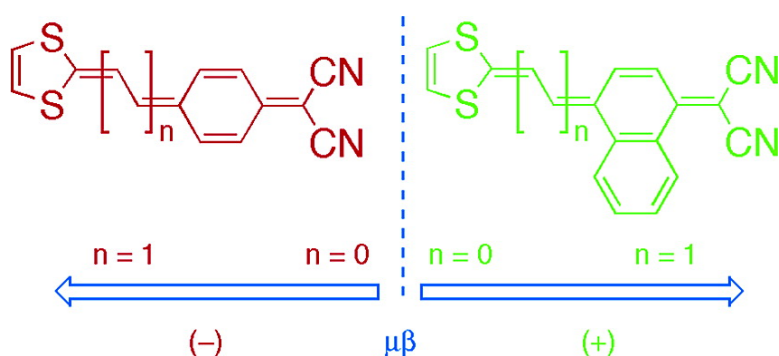


## Tuning First Molecular Hyperpolarizabilities through the Use of Proaromatic Spacers

Raquel Andreu, Maria Jess Blesa, Laura Carrasquer, Javier Garn, Jess Orduna, Beln Villacampa, Rafael Alcal, Juan Casado, Mari Carmen Ruiz Delgado, Juan T. Lopez Navarrete, and Magali Allain

*J. Am. Chem. Soc.*, **2005**, 127 (24), 8835-8845 • DOI: 10.1021/ja051819l • Publication Date (Web): 27 May 2005

Downloaded from <http://pubs.acs.org> on March 25, 2009



### More About This Article

Additional resources and features associated with this article are available within the HTML version:

- Supporting Information
- Links to the 19 articles that cite this article, as of the time of this article download
- Access to high resolution figures
- Links to articles and content related to this article
- Copyright permission to reproduce figures and/or text from this article

[View the Full Text HTML](#)

## Tuning First Molecular Hyperpolarizabilities through the Use of Proaromatic Spacers

Raquel Andreu,<sup>†</sup> Maria Jesús Blesa,<sup>†</sup> Laura Carrasquer,<sup>†</sup> Javier Garín,<sup>\*,†</sup> Jesús Orduna,<sup>†</sup> Belén Villacampa,<sup>‡</sup> Rafael Alcalá,<sup>‡</sup> Juan Casado,<sup>§</sup> Mari Carmen Ruiz Delgado,<sup>§</sup> Juan T. López Navarrete,<sup>§</sup> and Magali Allain<sup>||</sup>

Contribution from the Departamento de Química Orgánica-ICMA, Universidad de Zaragoza-CSIC; E-50009 Zaragoza, Spain, Departamento de Física de la Materia Condensada-ICMA, Universidad de Zaragoza-CSIC; E-50009 Zaragoza, Spain, Departamento de Química-Física, Facultad de Ciencias, Universidad de Málaga, 29071-Málaga, Spain, Laboratoire de Chimie, Ingénierie Moléculaire et Matériaux d'Angers (UMR CNRS 6200), Université d'Angers, 2, Boulevard Lavoisier 49045-Angers CEDEX, France

Received March 22, 2005; E-mail: jgarin@unizar.es

**Abstract:** In this paper, we describe the second-order nonlinear optical properties of a series of 1,3-dithiole-based electron donor–acceptor systems incorporating proaromatic donor and spacer groups. Modification of the proaromaticity of the quinoid spacer gives rise to NLO-phores with  $\mu\beta$  values ranging from  $-2000 \times 10^{-48}$  esu to  $+3000 \times 10^{-48}$  esu. Quite surprisingly, compounds with a *p*-benzoquinoid spacer and a strong acceptor group show negative  $\mu\beta$  values, usually associated to zwitterionic ground states, and yet they are largely quinoid, as evidenced by crystallographic data and theoretical calculations. Progressive benzoannulation of the spacer and introduction of alkylsulfanyl substituents on the dithiole donor unit result in a shift to more positive  $\mu\beta$  values. DFT and ab initio calculations verify these empirical trends.

### Introduction

A great deal of effort has been devoted to the synthesis of  $\pi$ -conjugated donor–acceptor (D–A) organic molecules in the search of new materials exhibiting second-order nonlinear optical (NLO) properties. This effort has allowed the determination of the structural features required to attain enhanced quadratic molecular responses, and the preparation of monomers and polymers with applications in molecular electronics and photonics.<sup>1</sup> Dipolar push–pull molecules constitute the widest class of compounds investigated for their NLO properties, and it is well-known that the first molecular hyperpolarizability ( $\beta$ ) depends not only on the strength of the donor and acceptor groups, but also on the nature of the  $\pi$ -conjugated spacer through which they interact. To that end, polyenic spacers have attracted much attention because the necessary intramolecular charge transfer (ICT) is greatly favored by such electron relays and, despite their limited stability, push–pull polyenes have been shown to display huge nonlinearities.<sup>2</sup>

On the other hand, aromatic spacers increase the stability of D– $\pi$ –A NLO-phores, but it was soon recognized that systems with predominantly aromatic ground states would not favor the ICT process, due to the concomitant loss of resonance stabilization accompanying the excitation from the neutral, aromatic ground state, to a zwitterionic, quinoid-like excited state. Thus, dipolar compounds with acceptors gaining aromaticity (“proaromatic”) on charge-transfer excitation were devised and the beneficial effect of this structural modification on the NLO properties of these systems was confirmed.<sup>2a,3</sup>

Following this line of reasoning, some push–pull compounds with both proaromatic D and A groups have been reported, showing either positive or negative  $\beta$  values, depending on the contribution of the zwitterionic and neutral limiting forms to the description of the ground state of these molecules.<sup>4</sup> In a similar vein, a few systems comprising proaromatic donors and proaromatic spacers (when depicted as their quinoid forms) have been prepared and shown to display large negative  $\beta$  values,

<sup>†</sup> Química Orgánica, Universidad de Zaragoza.

<sup>‡</sup> Física de la Materia Condensada, Universidad de Zaragoza.

<sup>§</sup> Universidad de Málaga.

<sup>||</sup> Université d'Angers.

(1) (a) *Materials for Nonlinear Optics: Chemical Perspectives*; Marder, S. R., Stucky, G. D., Sohn, J. E., Eds.; ACS Symposium Series, Vol. 455; American Chemical Society: Washington, DC, 1991. (b) *Organic Nonlinear Optical Materials*; Bosshard, Ch., Sutter, K., Prêtre, Ph., Hulliger, J., Flörshemer, M., Kaatz, P., Günter, P., Eds.; Advances in Nonlinear Optics, Vol. 1; Gordon & Breach: Amsterdam, 1995. (c) *Nonlinear Optics of Organic Molecules and Polymers*; Nalwa, H. S., Miyata, S., Eds.; CRC Press: Boca Raton, FL, 1997. (d) Wolf, J. J.; Wortmann, R. *Adv. Phys. Org. Chem.* **1999**, *32*, 121–217.

(2) (a) Marder, S. R.; Cheng, L.-T.; Tiemann, B. G.; Friedli, A. C.; Blanchard-Desce, M.; Perry, J. W.; Skindhøj, J. *Science* **1994**, *263*, 511–514. (b) Blanchard-Desce, M.; Alain, V.; Bedworth, P. V.; Marder, S. R.; Fort, A.; Runser, C.; Barzoukas, M.; Lebus, S.; Wortmann, R. *Chem. Eur. J.* **1997**, *3*, 1091–1104. (3) Marder, S. R.; Beratan, D. N.; Cheng, L.-T. *Science* **1991**, *252*, 103–106. (4) (a) Pan, F.; Wong, M. S.; Gramlich, V.; Bosshard, C.; Günter, P. *J. Am. Chem. Soc.* **1996**, *118*, 6315–6316. (b) Albert, I. D. L.; Marks, T. J.; Ratner, M. A. *J. Am. Chem. Soc.* **1997**, *119*, 3155–3156. (c) Albert, I. D. L.; Marks, T. J.; Ratner, M. A. *J. Am. Chem. Soc.* **1998**, *120*, 11174–11181. (d) Kay, A. J.; Woolhouse, A. D.; Gainsford, G. J.; Haskell, T. G.; Barnes, T. H.; McKinnie, I. T.; Wyss, C. P. *J. Mater. Chem.* **2001**, *11*, 996–1002. (e) Andreu, R.; Garín, J.; Orduna, J.; Alcalá, R.; Villacampa, B. *Org. Lett.* **2003**, *5*, 3143–3146.

Chart 1

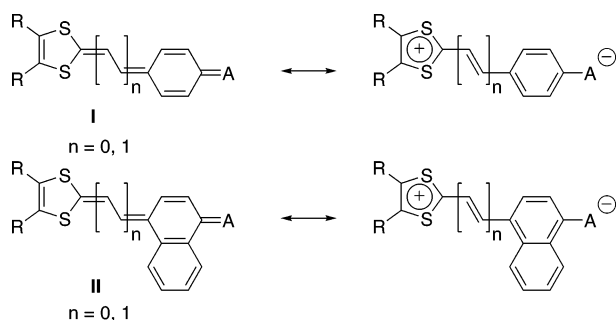
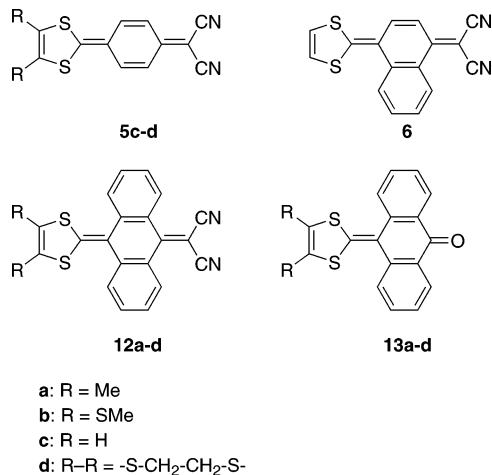


Chart 2

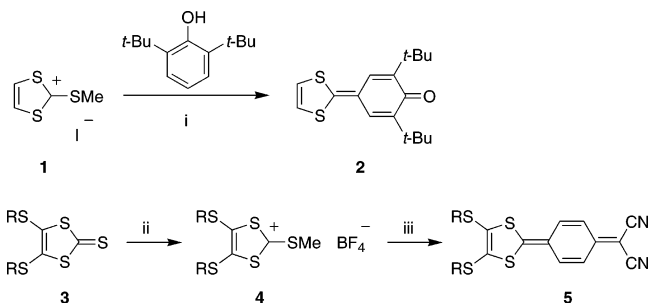


due to the fact that these molecules have largely zwitterionic ground states.<sup>5</sup>

Since the 1,3-dithiole moiety is an efficient donor group for new NLO-phores,<sup>4e,6</sup> in this work we study the second-order NLO properties of doubly proaromatic chromophores of general structures **I** and **II** (Chart 1), where a 1,3-dithiole unit and an electron-acceptor group are conjugated through a *p*-benzoquinoid spacer. These compounds make it possible to ascertain the effect that end groups, benzoannulation of the spacer and extension of the conjugation have on the structural (quinoidal vs. aromatic) and optical (magnitude and sign of  $\beta$ ) properties of these dyes.

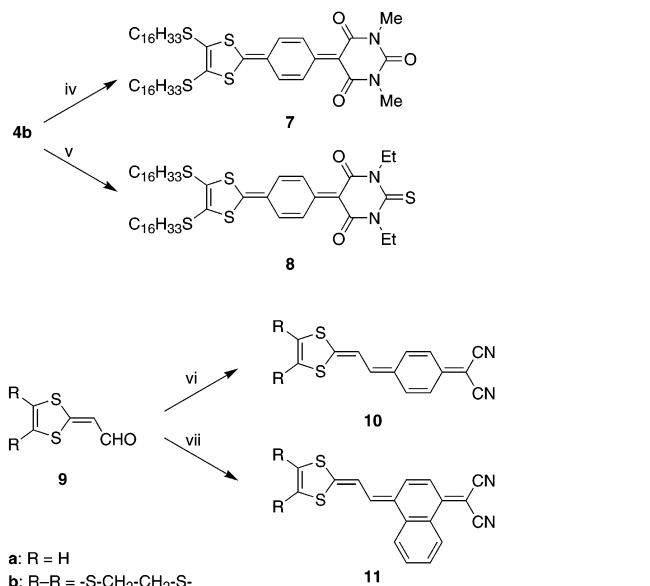
It should be noted that the first compounds of this type (**5c**, **6**, and **12c**) were prepared by Gompper,<sup>7</sup> and that the anthraquinoid series (compounds **12** and **13**) was later studied by Bryce (Chart 2).<sup>8</sup> A few other push-pull systems incorporating a 1,3-dithiol-2-ylidene and a diphenylquinoid or a heteroquinoid spacer have been described,<sup>9</sup> but, to the best of our knowledge, their second-order NLO properties have not been reported.

**Synthesis.** Compound **2** was prepared by reaction of **1**<sup>10</sup> with 2,6-di-*tert*-butylphenol (Scheme 1). Compounds **5** were prepared

Scheme 1<sup>a</sup>

a: R = C<sub>6</sub>H<sub>11</sub>

b: R = C<sub>16</sub>H<sub>33</sub>



<sup>a</sup> Reagents and conditions: (i) AcOH/py, reflux; (ii) (1) Me<sub>2</sub>SO<sub>4</sub> 100 °C; (2) AcOH, HBF<sub>4</sub>, Et<sub>2</sub>O; (iii) phenylmalononitrile, AcOH/py, reflux; (iv) 1,3-dimethyl-5-phenylbarbituric acid, AcOH/py, reflux; (v) 1,3-diethyl-5-phenylthiobarbituric acid, AcOH/py, reflux; (vi) phenylmalononitrile, Ac<sub>2</sub>O, py, 80 °C; (vii) 1-naphthylmalononitrile, Ac<sub>2</sub>O, py, 80 °C.

by reaction of phenylmalononitrile with the corresponding 2-methylsulfanyl-1,3-dithiolium salt. Due to the low solubility of compound **5c**,<sup>7</sup> some substituted derivatives incorporating aliphatic chains (**5a** and **5b**) were prepared. Thus, 1,3-dithiole-2-thiones **3a**<sup>11</sup> and **3b**<sup>12</sup> were converted to the corresponding 2-methylsulfanyl-1,3-dithiolium tetrafluoroborates **4** using a general procedure<sup>13</sup> with minor modifications. Compound **5a** bearing two pentylsulfanyl chains turned out to be much more soluble in common organic solvents than **5b** and, therefore, only the properties of the former were studied.

Compound **6** was prepared as previously described.<sup>7</sup>

Quinoid derivatives containing a barbituric-type acceptor, **7** and **8**, were prepared by the reaction of salt **4b** with the corresponding 5-phenylbarbituric (or thiobarbituric) derivative. It should be noted that only one compound (containing a 1,3-benzodithiole fragment) of type **7** has previously been described<sup>7</sup> and that our efforts to prepare compounds similar to **7** with the

(5) (a) Honeybourne, C. L. *J. Phys. D: Appl. Phys.* **1990**, *23*, 245–249. (b) Abbotto, A.; Beverina, L.; Bradamante, S.; Facchetti, A.; Klein, C.; Pagani, G. A.; Redi-Abshiro, M.; Wortmann, R. *Chem. Eur. J.* **2003**, *9*, 1991–2007.

(6) (a) Barzoukas, M.; Blanchard-Desce, M.; Josse, D.; Lehn, J.-M.; Zyss, J. *Chem. Phys.* **1989**, *133*, 323–329. (b) Jen, A. K.-Y.; Rao, V. P.; Drost, K. J.; Wong, K. Y.; Cava, M. P. *J. Chem. Soc., Chem. Commun.* **1994**, 2057–2058.

(7) Gompper, R.; Wagner, H.-U.; Kutter, E. *Chem. Ber.* **1968**, *101*, 4123–4143.

(8) Batsanov, A. S. et al. *Chem. Eur. J.* **1998**, *4*, 2580–2592.

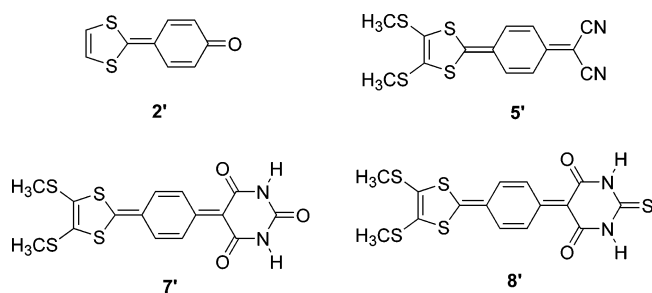
(9) (a) Inoue, S.; Aso, Y.; Otsubo, T. *Chem. Commun.* **1997**, 1105–1106. (b) Inoue, S.; Mikami, S.; Aso, Y.; Otsubo, T.; Wada, T.; Sasabe, H. *Synth. Met.* **1997**, *84*, 395–396.

(10) Challenger, F.; Mason, E. A.; Holdsworth, E. C.; Emmott, R. *J. Chem. Soc.* **1953**, 292–304.

(11) Simonsen, K. B.; Svenstrup, N.; Lau, J.; Simonsen, O.; Mørk, P.; Kristensen, G. J.; Becher, J. *Synthesis* **1996**, 407–418.

(12) Tormos, G. V.; Cava, M. P.; Wu, X.-L.; McKinley, A. J.; Metzger, R. M. *Synth. Met.* **1992**, *52*, 131–146.

(13) Moore, A. J.; Bryce, M. R. *Synthesis* **1991**, 26–28.

**Chart 3.** Model Compounds Used in Theoretical Calculations**Table 1.** B3P86/6-31G(d) Values for BLA ( $\delta r$ )<sup>a</sup>, Charge in the Dithiole Moiety, C–S Bond Distances<sup>b</sup>, and Quinoid Character ( $\chi_S$ )<sup>a</sup>

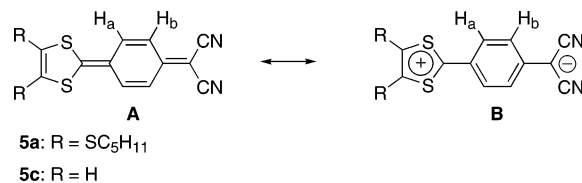
compound	$\delta r$	charge (e)	C–S (Å)	$\chi_S$ (%)
<b>2'</b>	0.101	+0.031	1.757	
<b>5c</b>	0.075	+0.094	1.750	92
<b>5c<sup>c</sup></b>	0.055	+0.344	1.729	73
<b>5'</b>	0.073	+0.115	1.741	93
<b>5'<sup>c</sup></b>	0.056	+0.332	1.724	73
<b>8'</b>	0.069	+0.155	1.737	

<sup>a</sup> See text. <sup>b</sup> C–S dithiole bonds adjacent to the exocyclic C=C bond. <sup>c</sup> In DMSO (PCM).

dithiole ring either unsubstituted or bearing two pentylsulfanyl chains failed.

The reaction of aldehydes **9a**<sup>14</sup> and **9b**<sup>13</sup> with phenyl- or 1-naphthylmalononitrile afforded extended derivatives **10** and **11**, respectively. To the best of our knowledge, the reaction of these arylmalononitriles with aldehydes had not been previously reported.

**Bond Length Alternation.** The bond length alternation (BLA) in the cyclohexadiene ring of compounds **I** ( $n = 0$ ) is a good indication for the charge transfer from the dithiole donor to the acceptor moiety. Quantitatively, BLA can be expressed by the degree of bond length alternation,  $\delta r$ , which equals 0 for benzene, whereas values between 0.08 and 0.12 are usually found in fully quinoid rings.<sup>15</sup> Not surprisingly, the presence of a weak electron acceptor results in a highly quinoid structure. Thus, model compound **2'** (Chart 3) shows (Table 1) a  $\delta r$  of 0.101 (*p*-benzoquinone exhibits a  $\delta r$  of 0.14, either using the experimentally determined bond lengths<sup>16</sup> or our calculated B3P86/6-31G(d) values). Stronger electron-withdrawing groups give rise to less alternated structures, as exemplified by the  $\delta r$  value of the B3P86/6-31G(d) geometry of compound **5c** (0.075). For the sake of comparison, tetracyanoquinodimethane (TCNQ) exhibits  $\delta r$  values of 0.08 (based on standard bond lengths),<sup>17</sup> 0.09 (B3P86/6-31G(d) geometry) or 0.10 (single-crystal structure).<sup>18</sup> Mulliken population analysis of these model compounds confirms these trends. The values obtained for the charges in the 1,3-dithiole units (Table 1) increase in the series **2'** < **5c**, indicating an increase in the degree of intramolecular charge transfer. Moreover, the progressive decrease along this series in the bond lengths of the dithiole C–S bonds adjacent to the

**Figure 1.** Limiting resonance structures of compounds **5**.

exocyclic double bond also supports the increased charge transfer, given the susceptibility of these bonds to the effective charge on the dithiole moiety.<sup>19</sup> Thus, all of these structural and electronic criteria indicate that the importance of the zwitterionic limiting form to the description of the ground state of these merocyanines increases in the order **2'** < **5c**. Moreover, the same trends are observed when comparing compounds **5'** and **8'** (Chart 3).

A comparison of **5c** and **5'** reveals that the effect of alkylsulfanyl substituents on the dithiole moiety on the ground state properties of these compounds is quite small. In every case, the introduction of two methylsulfanyl groups gives rise to the following: (a) slightly higher positive charges on the dithiole unit, (b) shorter C–S bond lengths, and (c) slightly less alternated structures (lower  $\delta r$  values) than those found in the corresponding unsubstituted compounds.

Moreover, given the dipolar nature of these compounds, the presence of a polar solvent should further stabilize the zwitterionic form, thus increasing the aromatic character of the spacer. This is confirmed through a comparison of the calculated geometries of **5c** in the gas phase and in DMSO ( $\epsilon = 46.7$ , polarized continuum model), which reveals a strong decrease of the  $\delta r$  value from 0.075 to 0.055 (Table 1) on inclusion of the solvent. Similar considerations apply to model compound **5'**. The modification in the quinoid character of these dicyanomethylene derivatives can also be expressed through their  $\chi_S$  parameters,<sup>17</sup> which are shown in Table 1 ( $\chi_S = 100\%$  for TCNQ). Moreover, Mulliken analysis of **5c** in DMSO shows that the positive charge on the dithiole ring (Table 1) and the negative charge on the C(CN)<sub>2</sub> group strongly increase when compared to the values of the gas-phase structure, whereas the charge borne by the cyclohexadiene ring remains nearly constant. Consequently, an increase in the zwitterionic character of these merocyanines is expected on increasing the polarity of the medium.

These conclusions are also supported by <sup>1</sup>H NMR spectral studies. To the best of our knowledge, the <sup>1</sup>H NMR spectrum of compound **5c** has not been previously reported. In DMSO-*d*<sub>6</sub> a singlet at  $\delta = 8.14$  is observed for the two dithiole hydrogen atoms, whereas the remaining hydrogen atoms appear as an A<sub>2</sub>X<sub>2</sub> system ( $\delta = 7.67$  and 6.88, respectively) with  $J = 9.0$  Hz. H<sub>a</sub> (Figure 1) was expected to be more deshielded than H<sub>b</sub>, since the latter should be closer to the partial negative charge present in the zwitterionic limiting form **B**.

This guess was confirmed by calculation of the isotropic shielding values in DMSO using the GIAO method at the PCM-B3P86/6-311+G(2d,p)//PCM-B3P86/6-31G(d) level, which showed that  $\delta H_a - \delta H_b = +0.62$ , in good agreement with the experimental value.

(14) Sugimoto, T.; Awaji, H.; Sugimoto, I.; Misaki, Y.; Kawase, T.; Yoneda, S.; Yoshida, Z.; Kobayashi, T.; Anzai, H. *Chem. Mater.* **1989**, *1*, 535–547.

(15) Dehu, C.; Meyers, F.; Brédas, J. L. *J. Am. Chem. Soc.* **1993**, *115*, 6198–6206.

(16) Van Bolhuis, F.; Kiers, C. Th. *Acta Crystallogr.* **1978**, *B34*, 1015–1016.

(17) Cole, J. C.; Cole, J. M.; Cross, G. H.; Farsari, M.; Howard, J. A. K.; Szablewski, M. *Acta Crystallogr.* **1997**, *B53*, 812–821.

(18) Long, R. E.; Sparks, R. A.; Trueblood, K. N. *Acta Crystallogr.* **1965**, *18*, 932–939.

(19) (a) Milián, B.; Ortí, E.; Hernández, V.; López-Navarrete, J. T.; Otsubo, T. *J. Phys. Chem. B* **2003**, *107*, 12175–12183. (b) Clemente, D. A.; Marzotto, A. *J. Mater. Chem.* **1996**, *6*, 941–946.

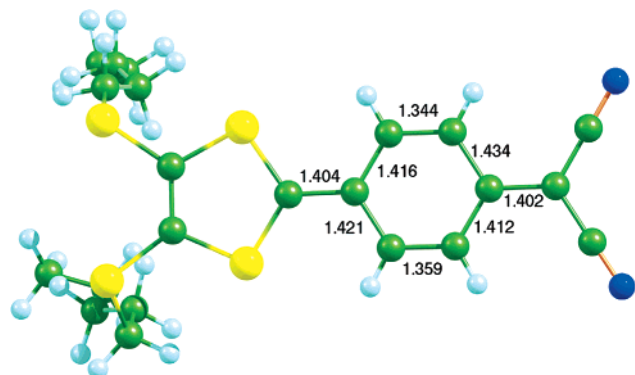


Figure 2. Selected bond lengths of **5a** in the solid state.

Although the limited solubility of **5c** precluded a comparative study of its  $^1\text{H}$  NMR spectra in different solvents, the use of the more soluble analogue **5a** revealed that on passing from  $\text{CDCl}_3$  to  $\text{DMSO}-d_6$  the doublet centered at  $\delta = 7.03$  was shifted to  $\delta = 6.91$ , whereas the doublet at  $\delta = 7.10$  was shifted to  $\delta = 7.57$ . This behavior supports the assignment of these signals to  $\text{H}_b$  and  $\text{H}_a$ , respectively, since limiting form **B** should contribute more to the description of the ground state of **5a** on increasing the polarity of the solvent, thus shifting protons  $\text{H}_b$  upfield and protons  $\text{H}_a$  downfield, the latter being more influenced by the developing positive charge in the dithiolium fragment. Moreover, this is consistent with previous observations on related donor–acceptor quinoid compounds.<sup>20</sup>

Similar structural considerations apply to extended derivatives **I** ( $n = 1$ ) with a *p*-benzoquinoid spacer; thus, the calculated  $\delta r$  values for compound **10a** in the gas phase and in  $\text{DMSO}$  are 0.076 and 0.055, respectively. These values are nearly identical to those of **5c** and therefore, also point to an important quinoid character of its ground state.

**Crystallographic Study of 5a.** Single crystals of **5a** suitable for X-ray analysis were grown from  $\text{CDCl}_3$  solution. According to the observed bond lengths (Figure 2), compound **5a** is moderately polarized in the solid state ( $\delta r = 0.069$ ,  $\chi_S = 79\%$ ), showing structural features intermediate between those calculated for model compound **5'** in the gas phase and in  $\text{DMSO}$ , respectively (Table 1). For **5a**, the experimentally determined  $\text{C}=\text{C}(\text{CN})_2$  bond length (1.402 Å) is considerably longer than that of the analogous bond in TCNQ (1.373 Å).<sup>21</sup> Concerning the donor end of the molecule, the exocyclic  $\text{C}=\text{CS}_2$  bond of **5a** is longer (1.404 Å) than the corresponding bond in previously reported structures where a 1,3-dithiolyliene and a dicyanomethylene groups are conjugated through oligoenic or (hetero)-aromatic spacers.<sup>22</sup> Not surprisingly, the lengthening of the exocyclic  $\text{C}=\text{CS}_2$  bond is accompanied by a marked shortening of the adjacent  $\text{C}-\text{S}$  bonds of **5a** (1.710 Å, averaged length). Taken together, these facts point to a noticeable degree of ICT in the ground state of **5a**, although the structure remains largely quinoid.

Figure 3 shows that the dithiole-quinoid group adopts a quasi planar geometry and lies in a plane orthogonal to that of the *S*-pentyl chains. In the molecular packing, the dithiole-quinoid

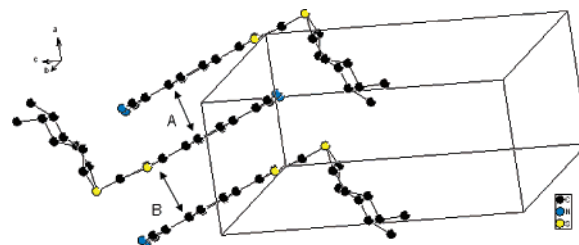


Figure 3. Details of molecular packing of **5a**.

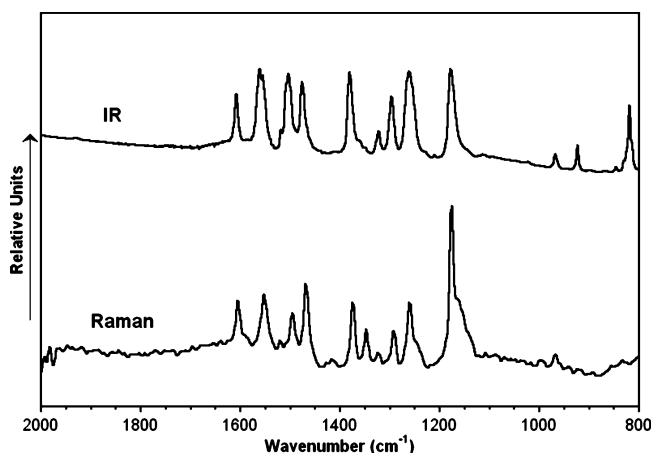


Figure 4. IR and Raman spectra of compound **10a**.

planes of the molecules stack along the *a* axis in a head-to-tail manner and form dimers with intradimer distances of  $A = 3.389(3)$  Å and interdimer distances of  $B = 3.499(3)$  Å.

Finally, it should be noted that the average of the X-ray determined bond lengths of the  $\text{C}-\text{S}$  dithiole bond adjacent to the exocyclic  $\text{C}=\text{C}$  bond is too short when compared to those obtained by B3P86/6-31G(d) calculations (Table 1). Despite the good performance of this hybrid functional at reproducing the geometry of organic sulfur compounds and TTF derivatives,<sup>23</sup> the calculated  $\text{C}-\text{S}$  bond lengths of TTF itself are longer (by ca. 0.02 Å) than those found by X-ray diffraction.<sup>24</sup>

To summarize, structural data and theoretical calculations show that the studied compounds have predominantly quinoid ground states, even in the polar crystalline environment or in solvents such as  $\text{DMSO}$ . This situation contrasts to that found in the related 7,7-diamino-8,8-dicyano-*p*-quinodimethanes, which have aromatic ground states.<sup>17,25</sup>

**Vibrational Infrared and Raman Spectra: Structural Analysis.** Compounds **5c**, **10a** and **11a** have been chosen to study the structural dependence of the molecular structure of the spacers upon D/A substitution by means of IR and Raman spectroscopies in solid state. Their IR and Raman spectra closely resemble each other, being this similarity especially large for the case of **10a** as observed in Figure 4. This phenomenon constitutes a proof of the existence of a great  $\text{D} \rightarrow \text{A}$  Intramolecular Charge Transfer (ICT) which is particularly effective in **10a**.<sup>26,27</sup>

- (20) (a) Morley, J. O.; Morley, R. M.; Docherty, R.; Charlton, M. H. *J. Am. Chem. Soc.* **1997**, *119*, 10192–10202. (b) Szablewski, M. et al. *J. Am. Chem. Soc.* **1997**, *119*, 3144–3154.  
 (21) Flandrois, S.; Chasseau, D. *Acta Crystallogr.* **1977**, *B33*, 2744–2750.  
 (22) (a) Moore, A. J. et al. *J. Mater. Chem.* **1998**, *8*, 1173–1184. (b) Moore, A. J. et al. *Eur. J. Org. Chem.* **2001**, 2671–2687. (c) Tomura, M.; Yamashita, Y. *Acta Crystallogr.* **2003**, *E59*, o1941–o1943.

- (23) (a) Altmann, J. A.; Handy, N. C.; Ingamels, V. E. *Mol. Phys.* **1997**, *92*, 339–352. (b) Viruela, R.; Viruela, P. M.; Pou-Américo, R.; Ortí, E. *Synth. Met.* **1999**, *103*, 1991–1992.  
 (24) Cooper, W. F.; Kenny, N. C.; Edmonds, J. W.; Nagel, A.; Wudl, F.; Coppens, P. *Chem. Commun.* **1971**, 889–890.  
 (25) Ravi, M.; Cohen, S.; Agrat, I.; Radhakrishnan, T. P. *Struct. Chem.* **1996**, *7*, 225–232.  
 (26) Hernández, V.; Casado, J.; Effenberger, F.; López Navarrete, J. T. *J. Chem. Phys.* **2001**, *112*, 5105–5112.

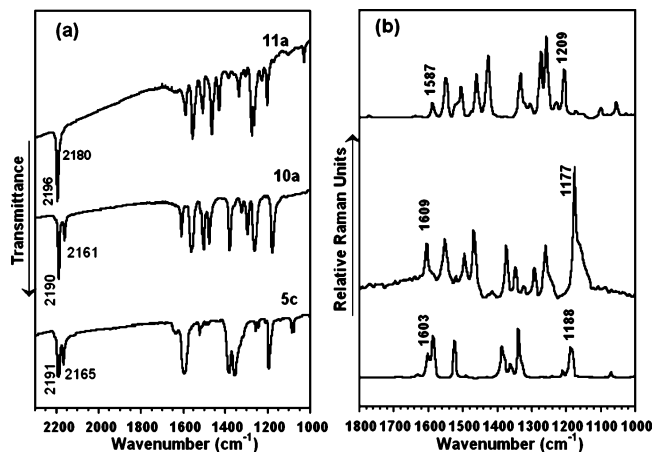


**Figure 5.** Comparison between the IR (a) and Raman (b) spectra of compounds **5c**, **10a** and **11a**.

The  $\pi$ -conjugated spacer, through which the D/A pair is connected, gives rise to some characteristic normal modes consisting of collective vibrations of the C=C/C–C conjugated path during which changes of the molecular polarizability (related to the absolute Raman intensity) are quite significant. In the case of D/A push–pull molecules, these Raman-active normal modes are also recorded with strong intensity in the IR spectrum because of the high charge polarization (charge flux and molecular dipole moment changes) of the same C=C/C–C backbone through which the charge transfer takes place.

Let us now closely inspect the spectra. The CN stretching vibration,  $\nu(\text{C}\equiv\text{N})$ , is observed for the three molecules as the strongest band of the spectra at around  $2190\text{ cm}^{-1}$  with a low-energy side component. Calculations predict this two-peaks structure, being the stronger one to be assigned to a normal mode in which the CN bonds vibrate in phase, while the second absorption at  $\sim 2160\text{ cm}^{-1}$  corresponds to the related out-of-phase motion. The frequency of the  $\nu(\text{C}\equiv\text{N})$  band is highly sensitive to the electron density borne by the nitrile groups and downshifts either upon complexation with electron donors or chemical/electrochemical reduction due to the lengthening of the C $\equiv$ N bonds.<sup>28</sup> Taking as a model reference a nonconjugated dicyano methane ( $\text{CH}_2(\text{CN})_2$ ), for which the  $\nu(\text{C}\equiv\text{N})$  band appears at  $2270\text{ cm}^{-1}$ , the significantly low frequencies (Figure 5) for the corresponding absorptions in our D-Spacer-A conjugated molecules  $2191$  and  $2165\text{ cm}^{-1}$  for **5c**,  $2190$  and  $2161\text{ cm}^{-1}$  for **10a**, and  $2196$  and  $2180\text{ cm}^{-1}$  for **11a** support the occurrence in the three systems of the already mentioned ICT toward the electron withdrawing C(CN)<sub>2</sub> group.<sup>29</sup> Moreover, the lowest values for **10a** suggest again that its degree of charge transfer is the greatest within the series. To further illustrate the phenomenon of the ICT, it must be noted that the symmetrically substituted TCNQ (7,7,8,8-tetracyanoquinodimethane) displays one intense IR absorption at  $2225 \pm 5\text{ cm}^{-1}$  in neutral state which evolves to  $2197\text{ cm}^{-1}$  for its radical anion and to  $2165\text{ cm}^{-1}$  for its dianion in which each dicyanomethylene group almost supports one negative charge.

Because we are analyzing a series of molecules with the same D/A pair, this trend shows that the  $\pi$ -conjugated spacer also contributes to the transferred electron density. Regarding **5c** the introduction of one more double-conjugated bond in **10a** improves the efficiency of the ICT, however, the contrary applies for the side attachment of a benzene group in **11a** likely due to the bifurcation of the electronic structure through a cross-conjugated path.

As for the Raman spectra in Figure 5 the bands around  $1600\text{ cm}^{-1}$  correspond to the C=C stretching vibration of the central six membered ring,  $\nu(\text{C}=\text{C})$ .<sup>30</sup> See Figure S2 in the supplementary information for the vibrational eigenvectors that support the assignments. This Raman line is measured at  $1609\text{ cm}^{-1}$  in **10a**, at  $1603\text{ cm}^{-1}$  in **5c** and at  $1587\text{ cm}^{-1}$  in **11a**. The Raman spectrum of liquid benzene displays an intense line at  $1607\text{ cm}^{-1}$  (mode 8a according to the Wilson's nomenclature) due to a mixed CCH deformation vibration,  $\beta(\text{CCH})$ , and CC stretching vibration,  $\nu(\text{CC})$ . This line shows a considerable downshift, up to  $1575\text{--}1580\text{ cm}^{-1}$ , with the *para*-substitution of benzene with electron acceptor groups which is interpreted in terms of gaining of quinoid character of this benzene ring as a consequence of the charge density withdrawal. Accordingly, for **5c** and **10a** with Raman lines at  $1603$  and  $1609\text{ cm}^{-1}$  respectively, it is reasonable to argue about the occurrence of a certain degree of aromatic character for their central six membered rings, more pronounced in the case of **10a**. As for **11a** the Raman line at  $1587\text{ cm}^{-1}$  denotes a larger degree of benzoquinoid character as compared with its two homologues. These spectroscopic data are in agreement with the solvatochromic and non linear optical behavior of these samples based in the consideration of partial polarization of the ground electronic state due to the presence of zwitterionic contributions (see Chart 1).

Further supporting the above sentence and in the low-medium energy region of the spectra there appear a group of bands that, from a structural point of view, have interesting implications. Again the Raman spectrum of aromatic benzene (liquid phase) shows a medium-intense line at  $1172\text{ cm}^{-1}$  which is due to mixed  $\beta(\text{CH})+\nu(\text{CC})$  vibration. Taking the Raman spectrum of TCNQ (7,7,8,8-tetracyanoquinodimethane) as a model molecule with a fully quinoid structure, it is observed the same mode to appear at  $1209\text{ cm}^{-1}$ . Finally the Raman frequency for the same vibration at  $1181\text{ cm}^{-1}$  in the spectrum of *p*-benzoquinone provides us with a more reference point for the sake of comparison. The trend for this Raman line in our three samples,  $1188\text{ cm}^{-1}$  in **5a**,  $1177\text{ cm}^{-1}$  in **10a**, and  $1207\text{ cm}^{-1}$  in **11a**, seems to corroborate the above-described interplay between pro-aromatic and pro-quinoid forms describing the ground electronic state of these chromophores.

The band at  $1525\text{ cm}^{-1}$  in **5c** is an exclusive  $\nu(\text{C}=\text{C})$  vibration of the dithiole group.<sup>30</sup> This band can be related to the weak line at  $1520\text{ cm}^{-1}$  in **10a** and to the group or progression of bands starting at  $1523\text{ cm}^{-1}$  in **11a** which, contrary to **5c** is largely mixed with the  $\nu(\text{C}=\text{C})$  vibration of the vinylenic bond linked to the central six membered ring. This last  $\nu(\text{C}=\text{C})$  mode appears associated with lines at higher frequencies:  $1553\text{ cm}^{-1}$  in **10a** and  $1550\text{ cm}^{-1}$  in **11a**. Theory predicts the double bond distances of the dithiole group to

(27) González, M.; Segura, J. L.; Seoane, C.; Martín, N.; Garín, J.; Orduna, J.; Alcalá, R.; Villacampa, B.; Hernández, V.; López Navarrete, J. T. *J. Org. Chem.* **2001**, *66*, 8872–8882.

(28) Taylor, R.; Kennard, O. *J. Am. Chem. Soc.* **1982**, *104*, 5063–5070.

(29) (a) Takenaka, T. *Spectrochim. Acta A* **1971**, *27*, 1735. (b) Girlando, A.; Pecile, C. *Spectrochim. Acta A* **1973**, *29*, 1859. (c) Khatkale, M. S.; Devlin, J. P. *J. Chem. Phys.* **1979**, *70*, 1851.

(30) Wartelle, C.; Viruela, R.; Viruela, P. M.; Sauvage, F. X.; Sallé, M.; Ortí, E.; Levillain, E.; Le Derf, F. *Phys. Chem. Chem. Phys.* **2003**, *5*, 4672–4679.

**Table 2.** Redox Potentials,  $\lambda_{\text{max}}$ ,  $E_{\text{g}}$ ,  $\mu\beta$ , and  $\mu\beta(0)$  Values of the Prepared Compounds

compound	$E_{\text{ox}}$ (V) <sup>a</sup>	$E_{\text{red}}$ (V) <sup>a</sup>	$\lambda_{\text{max}}$ (nm)		$E_{\text{g}}$ (eV)	$\mu\beta$ ( $10^{-48}$ esu)		$\mu\beta(0)$ ( $10^{-48}$ esu) <sup>b</sup>	
			(CH <sub>2</sub> Cl <sub>2</sub> )	(DMSO)		(CH <sub>2</sub> Cl <sub>2</sub> )	(DMSO)	(CH <sub>2</sub> Cl <sub>2</sub> )	(DMSO)
<b>2</b>	1.00	−1.66	492	503	2.40	95	64	68	45
	1.05 <sup>c</sup>	−1.36 <sup>c</sup>							
<b>5a</b>	0.88	−0.78	658	652	1.78	100	103	47	48
<b>5c</b>	0.87 <sup>c</sup>	−0.65 <sup>c</sup>	644	625	1.84	<i>d</i>	−635	<i>d</i>	−325
<b>6</b>	0.83	−0.86	607	628	1.87	−23	13	−13	7
	0.94 <sup>c</sup>	−0.60 <sup>c</sup>							
<b>7</b>	1.01, 1.46	−0.34	680	<i>d</i>	1.66	−270	<i>d</i>	−115	<i>d</i>
<b>8</b>	0.92	−0.50	700	<i>d</i>	1.63	−300	<i>d</i>	−120	<i>d</i>
<b>10a</b>	0.63	−0.64	759	742	1.53	<i>d</i>	−2000	<i>d</i>	−667
	0.66, 1.13 <sup>c</sup>	−0.46 <sup>c</sup>							
<b>10b</b>	<i>d</i>	<i>d</i>	781	786	1.48	<i>d</i>	<i>d</i>	<i>d</i>	<i>d</i>
<b>11a</b>	0.74	−0.63	652 <sup>e</sup>	754	1.56	2500	355	1180	115
	0.74 <sup>c</sup>	−0.46 <sup>c</sup>							
<b>11b</b>	0.80	−0.58	672 <sup>e</sup>	770	1.51	3100	<i>d</i>	1366	<i>d</i>

<sup>a</sup> In CH<sub>2</sub>Cl<sub>2</sub>, vs Ag/AgCl, glassy carbon working electrode, 0.1 M Bu<sub>4</sub>NPF<sub>6</sub>, 0.1 V s<sup>−1</sup>. Ferrocene internal reference  $E_{1/2}$  = 0.47 V. <sup>b</sup> Values calculated using the two-level model. <sup>c</sup> In DMF. Ferrocene internal reference  $E_{1/2}$  = 0.57 V. <sup>d</sup> Too low solubility. <sup>e</sup> See text.

scarcely change in the series of compounds which supports the slight affectation of their associated vibrational frequencies upon increasing gaining of ICT character on going from **11a** to **5c** and finally to **10a**.

**Electrochemical and Linear Optical Studies.** The studied compounds show one oxidation wave (two in some cases) and one irreversible reduction wave, which can be attributed to the donor and the acceptor moieties, respectively (Table 2). It can be seen that compounds with stronger acceptors (**7** and **8**) show less negative reduction potentials than those of derivatives with weaker acceptors (**5a**). Accordingly, the oxidation potential of **5a** is lower than that of **7** or **8**. The surprisingly high oxidation potential of **2**, bearing the weakest acceptor, can be attributed to the poor solvation of its cation-radical, maybe due to the steric effect of the two *tert*-butyl groups. The presence of an additional C=C double bond in the spacer (cf. **5c** and **10a**, or **6** and **11a**) gives rise to a lowering of the oxidation potentials and to a shift of  $E_{\text{red}}$  to less cathodic values, which is due to the increased stabilization of the corresponding cation-radicals and anion-radicals, respectively, because of the extended conjugation. Benzoannulation of the spacer has the effect of increasing the corresponding  $E_{\text{ox}}$  values, both in the dithiolyliidencyclohexadiene series (cf. compounds **5c** and **6** in DMF or **6** and **12c**<sup>8</sup> in CH<sub>2</sub>Cl<sub>2</sub>) and in the series of compounds with extended conjugation (cf. **10a** and **11a**). A similar trend has previously been noted in the case of extended tetrathiafulvalenes incorporating benzo-, naphtho-, and anthraquinoid spacers.<sup>31</sup>

All of the studied compounds show an intense band in the visible region. The wavelengths of the maxima of the lowest energy absorption and the optical gaps,  $E_{\text{g}}$ , (estimated from the tangent to the low energy edge of the absorption band) are gathered in Table 2. The effect of the acceptor on the optical properties can be ascertained either comparing compound **2** to **5c** or in the series **5a**, **7**, **8**. Stronger acceptors cause a bathochromic shift of the lowest energy absorption band that is also reproduced by TD-DFT calculations. Molecules with stronger acceptors have, in general, a lower energy LUMO and therefore a reduced HOMO–LUMO gap. In fact, there is an excellent agreement between the trends shown by the calculated

HOMO–LUMO gaps (Gap<sub>HL</sub> in Table 3) and the optical gaps (Table 2) for all of the studied compounds.

Although the limited solubility of these derivatives has precluded a full comparative study, it should be noted that whereas **2** shows a positive solvatochromism, the inverse holds for compound **5c**, as previously noted for closely related derivatives.<sup>9a,32</sup> These facts reflect the increased zwitterionic character of **5c** when compared to **2**, in agreement with the structural and electronic features discussed above.

Comparison of compounds **5c**, **6**, and **12c** reveals that increasing the number of fused benzene rings in the spacer produces a marked hypsochromic shift of the lowest energy absorption in CH<sub>2</sub>Cl<sub>2</sub>.<sup>33</sup> This phenomenon can be explained on the basis of the increased HOMO–LUMO gaps calculated by DFT (2.42 eV for **5c**, 2.57 eV for **6**, and 2.74 eV for **12c**). Quite surprisingly, TD-DFT calculations fail to predict this trend.

The UV–vis spectra of compounds **11a** and **11b** in CH<sub>2</sub>Cl<sub>2</sub> show very broad absorptions, extending from ca. 500 nm to 800 nm, with maxima at 652 and 672 nm, respectively (see Table 2). In the case of **11a**, deconvolution of the spectrum reveals the presence of three maxima at 601, 660, and 726 nm. On the other hand, the spectrum of **11b** in CH<sub>2</sub>Cl<sub>2</sub> is completely featureless, precluding a deconvolution study. Despite these limitations, the hypsochromic shift due to benzoannulation is also noticeable in the series of compounds with extended conjugation (cf. **10a** and **11a**). Again in this series an increased HOMO–LUMO gap is predicted for the benzoannulated derivative, although TD-DFT calculations erroneously predict a bathochromic shift on passing from **10a** to **11a**. Benzoannulation also affects the solvatochromic behavior of these systems, as can be deduced from the negative solvatochromism of **5c** and **10a** and the positive behavior of the corresponding naphthoquinoid derivatives **6** and **11a**, respectively.

As expected, the inclusion of an additional CH=CH group between the 1,3-dithiole and the quinoid spacer causes a marked bathochromic shift of the lowest energy band (compare **5c** to **10a**, **5a** to **10b**, and **6** to **11a**). This effect is correctly reproduced by TD-DFT calculations. The extension of conjugation causes

(31) (a) Martín, N.; Sánchez, L.; Seoane, C.; Ortí, E.; Viruela, P. M.; Viruela, R.; *J. Org. Chem.* **1998**, *63*, 1268–1279. (b) Yamashita, Y.; Kobayashi, Y.; Miyashi, T. *Angew. Chem., Int. Ed. Engl.* **1989**, *28*, 1052–1053.

(32) Gompper, R.; Kutter, E.; Wagner, H.-U. *Angew. Chem., Int. Ed.* **1966**, *5*, 517–518.

(33) Gompper, R.; Wagner, H.-U. *Tetrahedron Lett.* **1968**, 165–169.

**Table 3.** Results of Theoretical Calculations<sup>a</sup>

compound	solvent <sup>b</sup>	B3P86/6-31G(d)						HF/6-31G(d)		
		Gap <sub>H-L</sub> (eV)	E (eV)	$\mu_g$ (D)	$\mu_e$ (D)	$\Delta\mu_{ge}$ (D)	<i>f</i>	$\mu_g$ (D)	$\beta_{tot}(0)^c$	$\mu\beta(0)^d$
2'		3.17	3.36	8.3	12.2	3.9	0.61	8.46	0.3	2.6
5c		2.42	2.79	13.6	13.0	-0.6	1.04	14.6	32.0	-467
5'	DMSO	2.27	2.48	24.2	17.8	-6.4	1.12	13.22	28.6	-377
	CH <sub>2</sub> Cl <sub>2</sub>		2.42	13.4	23.5	10.1	0.82			
6	DMSO	2.57	2.16	18.3	20.9	2.6	1.11	12.07	4.5	5.8
	CH <sub>2</sub> Cl <sub>2</sub>		2.19	22.5	25.7	3.2	1.06			
7'	DMSO	2.28	2.69	12.3	17.6	5.3	0.70	11.90	42.9	-510
	CH <sub>2</sub> Cl <sub>2</sub>		2.42	20.2	20.6	0.4	0.93			
8'		2.20	2.37	11.8	19.7	7.9	0.93	14.51	77.6	-1126
10a	DMSO	2.14	2.28	14.2	15.6	1.4	1.14	16.56	23.3	-346
	CH <sub>2</sub> Cl <sub>2</sub>		2.55	15.6	16.8	1.2	1.52			
10b	DMSO	2.10	2.22	26.9	21.6	-5.3	1.62	18.08	17.6	-245
	CH <sub>2</sub> Cl <sub>2</sub>		2.19	26.7	22.5	-4.2	1.58			
11a	DMSO	2.20	2.37	17.8	28.2	10.4	1.34	14.66	34.8	408
	CH <sub>2</sub> Cl <sub>2</sub>		2.46	14.4	21.6	7.2	1.17			
11a(C <sub>s</sub> )	DMSO	2.12	2.15	24.3	25.7	1.4	1.44	14.83	31.0	343
	CH <sub>2</sub> Cl <sub>2</sub>		2.12	26.8	26.6	-0.2	1.46			
11b		2.26	2.47	14.6	21.6	7.0	1.19	15.85	48.4	665
12c		2.74	2.30	16.3	29.9	13.6	1.09	8.70	8.5	69
12c(C <sub>2v</sub> )		2.74	2.37	8.6	22.3	13.7	0.18	12.58	12.7	160
			2.54	12.4	23.3	8.9	0.44			

<sup>a</sup> Calculations on geometries optimized at the B3P86/6-31G(d) level. Geometry optimizations were performed without restrictions unless otherwise stated. <sup>b</sup> Solvent calculations used the PCM model. <sup>c</sup> In 10<sup>-30</sup> esu. <sup>d</sup> In 10<sup>-48</sup> esu.

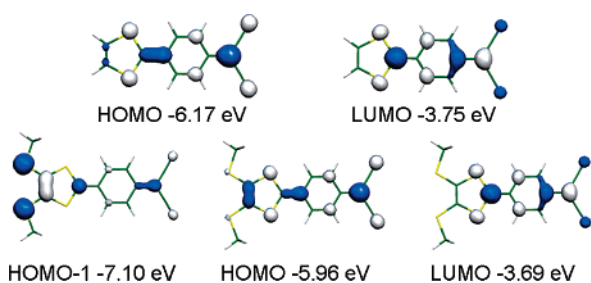


**Figure 6.** Illustration of the 0.05 contour surface diagrams of the molecular orbitals of **5c** (top) and **5'**.

an increased energy of the HOMO and a lowering of the energy of the LUMO and, consequently, a decreased HOMO–LUMO gap.

The presence of alkylsulfanyl substituents on the dithiole ring results in a bathochromic shift of the lowest energy absorption (cf. **5a** and **5c**, or **10a** and **10b**), as is usually the case for dithiafulvene derivatives. This effect is also reproduced theoretically (see Table 3). Alkylsulfanyl donor groups increase the energy of both the HOMO and the LUMO, but this effect is stronger on the HOMO energy (see Figure 6) and, therefore, there is a decreased HOMO–LUMO gap that is reflected in the observed bathochromic shift. A comparison of the solvatochromic behavior of **5a** and **5c** (or **10a** and **10b**) shows that the *S*-linked substituents give rise to positive (or less negative) solvatochromism. As discussed below, this effect has important consequences on the NLO properties of these molecules.

**Nonlinear Optics.** The second-order NLO properties of the Gompper-type molecules described in this work have not been measured previously, except for the fact that compound **5c** was reported (without details) to have a very low  $\beta$  value ( $<1.10^{-30}$  esu).<sup>34</sup>

The nonlinear optical properties determined by the EFISHG technique are gathered on Table 2. To rationalize the nonlinear

optical behavior of these compounds we have also performed theoretical calculations on some of the synthesized compounds as well as the model compounds shown in Chart 3.

Molecular hyperpolarizabilities have been estimated using the CPHF (Coupled Perturbed Hartree–Fock) method which involves the calculation of the analytical second derivative of the dipole moment with respect to the applied electric field. We have also calculated the parameters involved in the two level model ( $\beta(0) \propto \Delta\mu_{ge}^2/E^3$ , where  $\Delta\mu_{ge}$  is the difference between the excited and ground-state dipole moments,  $\mu_e$  and  $\mu_g$  respectively, *f* is the oscillator strength and *E* the excitation energy) by TD-DFT (Time Dependent Density Functional Theory) in order to obtain a more intuitive description of the observed trends in the nonlinear optical behavior of the studied compounds and finally, these parameters have been also calculated in solution using a PCM model with aims to understand the effect of the solvent on the nonlinear optical properties. A summary of the results of these calculations is gathered in Table 3.

While TD-DFT is the more accurate method that can be applied to study the excited states of large molecules at an affordable computational cost, these calculations present as a drawback the poor description of charge-transfer transitions.<sup>35</sup> Furthermore, it can be seen that the agreement between calculated and theoretical hyperpolarizabilities is only limited, probably due to the fact that solvent effects were not considered in CPHF calculations. Although theoretical calculations do not provide accurate values to be directly compared to experimental ones, both TD-DFT and CPHF are useful tools in order to explain the experimental trends discussed below.

As a rule, most of the nonlinear optical response is associated to the lowest energy allowed absorption which according to TD-DFT calculations is mainly contributed from the HOMO–LUMO transition. However, contrary to previously reported

(34) Staring, E. G. J. *Recl. Trav. Chim. Pays-Bas* **1991**, *110*, 492–506.

(35) (a) Tozer, D. J.; Amos, R. D.; Handy, N. C.; Roos, B. O.; Serrano-Andres, L. *Mol. Phys.* **1999**, *97*, 859–868. (b) Dreuw, A.; Head-Gordon, M. *J. Am. Chem. Soc.* **2004**, *126*, 4007–4016.

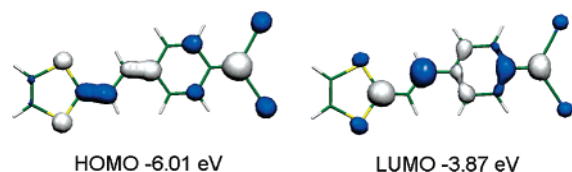


**Figure 7.** Illustration of the 0.05 contour surface diagrams of the HOMO and LUMO of **10a**.

dithiole- and tetrathiafulvalene NLO-phores which have the HOMO located on the donor unit and the LUMO on the acceptor, the HOMO and LUMO of most of the studied compounds spread over the whole molecule in such a way that the lowest energy transition can be hardly considered as a charge-transfer process (see Figure 7). As a result of this electronic configuration, excitation from the ground to the excited state does not always result in an increased dipole moment and hence a positive hyperpolarizability. In other words, the contribution of the zwitterionic form is for some molecules higher in the ground state than in the excited state and thus, these molecules show a negative hyperpolarizability.

The effect caused by different structural modifications on the optical properties of these chromophores will be discussed separately.

**Acceptor Strength.** Compound **5c**, with a stronger acceptor than **2**, shows a larger value of  $|\mu\beta(0)|$ . The negative  $\mu\beta(0)$  value of the former is in good agreement with the observed negative solvatochromism. Increasing the acceptor strength causes more negative hyperpolarizabilities as is also confirmed by the CPHF calculations. An explanation to this behavior can be found in the ground and excited-state dipole moments calculated by TD-DFT. The difference  $\mu_e - \mu_g$  is 3.9 D for **2'** and  $-0.6$  D for **5c**. In other words, strong acceptors make these molecules approach or even surpass the cyanine limit giving rise to negative hyperpolarizabilities. It should be noted that previous ZINDO/S calculations on compound **5c** erroneously predict that  $\mu_e - \mu_g > 0$ , which should give rise to positive  $\beta$  values.<sup>36</sup>

In a similar vein, there is an increase toward more negative  $\mu\beta(0)$  values on passing from **5a** to the (thio)barbituric acid derivatives **7** and **8**.

An interesting point arises when the structural and NLO properties of these compounds are taken into account. As discussed above, all these compounds are largely quinoid and yet, show negative  $\beta$  values (except for **5a**, see below). This situation contrasts to that found in pyridinium tricyanoquinodimethanides, which also display negative  $\beta$  values,<sup>5a</sup> but have aromatic ground states, as evidenced by X-ray diffraction<sup>37</sup> and theoretical calculations.<sup>38</sup> Therefore, the present compounds are not easy to classify as belonging to the left or right-hand side of Marder's curve, unlike their 7,7-diamino-8,8-dicyano-*p*-quinodimethane analogues.<sup>39</sup>

This apparently intriguing situation can be easily understood keeping in mind that the latter compounds are strongly polarized in their ground states, which are essentially zwitterionic and aromatic<sup>17,25</sup> whereas, on account of their negative hyperpolar-

**Table 4.** Nonlinear Optical Parameters of Anthraquinoid Derivatives **12** and **13**<sup>a</sup>

compound	$\mu\beta$ ( $10^{-48}$ esu)	$\mu\beta(0)$ ( $10^{-48}$ esu) <sup>b</sup>
<b>12c</b>	117	73
<b>12d</b>	166	99
<b>13c</b>	85	60
<b>13d</b>	127	88

<sup>a</sup> In  $\text{CH}_2\text{Cl}_2$ . <sup>b</sup> Values calculated using the two-level model.

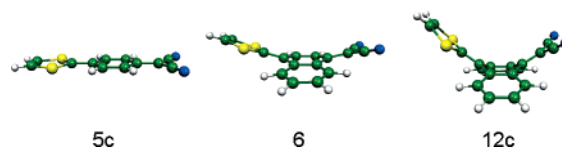


**Figure 8.** B3P86/6-31G(d) Calculated geometries of compounds **5c**, **6** and **12c**.

izability values, their excited states must be neutral and quinoid-like. For the compounds herein described the ground state is mainly quinoidal but, on passing from the ground to the excited state a further decrease in the zwitterionic character (and therefore, negative  $\beta$  values) are also expected. Thus, there is no qualitative difference between the behavior displayed by 7,7-diamino-8,8-dicyanoquinodimethane analogues and compounds such as **5c**, the enhanced ground-state polarization of the former arising from the stronger electron-donating ability of nitrogen atoms compared to that of sulfur atoms.

**Nature of the Spacer.** To study the effect of benzoannulation on the NLO properties of these systems, we have also measured the  $\mu\beta$  values of related derivatives<sup>8</sup> with anthraquinoid spacers (Table 4). The addition of fused benzene rings to the quinoid system modifies dramatically the non linear optical behavior of the studied molecules.

While compound **5c** displays a large negative hyperpolarizability, the naphthoquinoid derivative **6** has a very low nonlinear response and the addition of a new fused benzene ring in **12c** gives rise to a positive  $\mu\beta$  value and, similarly, the hyperpolarizability changes from negative to positive on passing from **10a** to **11a**. We can conclude that the addition of fused benzene rings leads to more positive hyperpolarizabilities and this trend is also predicted by the CPHF calculations shown in Table 3. A tentative explanation to this behavior could rely on the different geometry displayed by these NLO-phores (see Figure 8): while **5c** is completely planar ( $C_{2v}$  symmetry) there is some folding in **6** which has the dithiole ring and the dicyanomethylene acceptor above the quinoid ring plane and the fused benzene ring below that plane. The geometry of **12c** is even more folded adopting a butterfly-like geometry.<sup>8</sup>

Nevertheless, we have optimized the geometry of **12c** restricted to a planar ( $C_{2v}$ ) symmetry and have calculated the molecular hyperpolarizability using this geometry (see Table 3). To our surprise, the hyperpolarizability calculated at the planar geometry is even more positive than that obtained using the butterfly arrangement, so that the molecular shape is not responsible for the changes in the hyperpolarizability in this case. In a similar way we have calculated the hyperpolarizability of **11a** using a planar ( $C_s$ ) geometry (Table 3). Although the calculated  $\mu\beta(0)$  value is in this instance lower than that obtained without geometry restrictions, it is still positive in contrast to the negative  $\mu\beta(0)$  value calculated for **10a**.

(36) Sato, N.; Sakuma, T.; Yoshida, H.; Silinsh, E. A.; Jurgis, A. J. *Mol. Cryst. Liq. Cryst.* **2001**, *355*, 319–329.

(37) Metzger, R. M.; Heimer, N. E.; Ashwell, G. J. *Mol. Cryst. Liq. Cryst.* **1984**, *107*, 133–149.

(38) Kwon, O.; McKee, M. L.; Metzger, R. M. *Chem. Phys. Lett.* **1999**, *313*, 321–331.

(39) Cole, J. M.; Copley, R. C. B.; McIntyre, G. J.; Howard, J. A. K.; Szablewski, M.; Cross, G. H. *Phys. Rev. B* **2002**, *65*, 125107.

With geometrical parameters having little effect on the nonlinear optical properties, the different behavior of these compounds must be due to the different proaromaticity of the quinoid bridge. The more proaromatic quinoid ring in **5c** favors the zwitterionic form and this compound surpasses the cyanine limit and displays a negative hyperpolarizability. The less proaromatic spacer in **12c** favors the neutral form over the zwitterionic one and this molecule displays a positive  $\mu\beta(0)$ , compound **6** showing an intermediate behavior near the cyanine limit with a very low nonlinear optical response. The different charge transfer of these compounds is also reflected in the calculated ground-state dipole moments that decrease in the order **5c** > **6** > **12c**, and **10a** > **11a**. The trends in the nonlinear optical behavior are also reflected in the calculated dipole moments difference  $\Delta\mu_{ge}$  that increase with the number of fused benzene rings. Although the effect of benzoannulation of the spacer on NLO properties has not been previously studied, similar conclusions have been drawn from a series of strongly zwitterionic chromophores containing proaromatic donor units.<sup>5b</sup>

The nonlinear optical behavior of these compounds is also dramatically affected by the length of the conjugated spacer. The inclusion of a (CH)<sub>2</sub> group between the dithiole and quinoid groups causes a large increase in the absolute value of the hyperpolarizability. While CPHF calculations reproduce this trend on passing from compound **6** to **11a**, this is not the case when comparing **5c** to **10a** probably due to solvent effects that are not considered in the calculation but have an important influence on the nonlinear optical activity (see for example the effect of solvent on the  $\mu\beta$  value of **11a**). A more intuitive explanation of the effect of lengthening the spacer on the molecular hyperpolarizability can be extracted from TD-DFT calculations. Comparing the calculated values of **5c** to **10a**, **5a** to **10b**, and **6** to **11a** it can be seen that the variation of the calculated  $\Delta\mu_{ge}$  is not large enough to explain the changes in  $\beta$ . We must therefore focus on the other parameters involved in the two state level equation and we can see that the extended conjugation gives rise to a bathochromic shift and an increased oscillator strength for the lowest energy absorption, and the variation of both parameters results in larger hyperpolarizabilities.

**Substituents on the Dithiole Ring.** A comparison of **5c** to **5a** and **11a** to **11b** reveals that the presence of alkylsulfanyl substituents on the dithiole rings results in a more positive hyperpolarizability and these trends are also reproduced by our theoretical calculations (see Table 3). CPHF calculations predict a more positive hyperpolarizability for the alkylsulfanyl-substituted compounds compared to the unsubstituted ones, but a more intuitive picture can be obtained from TD-DFT calculations. If we compare the excitation energies and the calculated oscillator strengths of compounds **5c** and **5a** (or **5'** in the calculations), then the difference is not large enough to explain the dramatic change in the hyperpolarizability; therefore, the different hyperpolarizabilities must be due to differences in  $\Delta\mu_{ge}$  for these compounds. DFT calculations show that the ground state dipole moment is nearly insensitive to the presence of alkylsulfanyl substituents (calculated 13.6 and 13.4 D for **5c** and **5'** respectively) but there is a dramatic change in the excited state dipole moment (from 13.0 to 23.5 D). According to TD-DFT calculations the lowest energy absorption in **5c** can be considered as a pure HOMO  $\rightarrow$  LUMO transition but the

analogous absorption in **5'** has a significant contribution from the HOMO-1  $\rightarrow$  LUMO transition. Considering that the HOMO-1 is largely contributed from the substituent sulfur atoms (Figure 6) we can conclude that there is a considerable charge transfer from these atoms to the acceptor on excitation and therefore **5'** displays a larger excited-state dipole moment and a more positive hyperpolarizability than **5c**. These results contrast to those previously obtained by ZINDO/S calculations, which indicate that compounds **5c** and **5d** should have  $\beta$  values of the same sign.<sup>36</sup>

A similar conclusion can be drawn when comparing **10a** and **11a** to **10b** and **11b** respectively. In these instances, alkylsulfanyl groups cause a moderate increase in the ground state dipole moment but a largely increased excited state dipole moment and consequently a larger  $\Delta\mu_{ge}$  and a more positive hyperpolarizability.

Similarly, the introduction of alkylsulfanyl groups in the anthraquinoid series gives rise to more positive  $\mu\beta(0)$  values (Table 4).

## Conclusions

NLO-phores containing two proaromatic moieties (a 1,3-dithiole donor unit and a spacer incorporating a *p*-quinoid fragment) have been synthesized, and the effect of varying the proaromaticity of the spacer through benzoannulation on their second-order NLO properties has been studied for the first time. Provided that strong electron acceptors are used, compounds with a *p*-benzoquinoid spacer display negative  $\mu\beta$  values, which become progressively more positive on passing to the naphtho- and then to the anthraquinoid derivatives. This is consistent with a smaller contribution of the zwitterionic limiting form to the description of the ground state of these molecules on increasing the number of fused benzene rings. IR and Raman spectra also indicate a lesser degree of ICT on benzoannulation. It is worth noting that, according to X-ray diffraction data and theoretical calculations, even the NLO-phores showing negative  $\mu\beta$  values have predominantly quinoid ground states. This fact precludes a clear-cut classification of these molecules as belonging either to the left- or right-hand side of Marder's curve. Peripheral sulfur atoms on the dithiole ring have a very important effect on the excited state properties, giving rise to more positive hyperpolarizabilities when compared to their unsubstituted analogues. The inclusion of an additional ethylenic unit in the spacer greatly amplifies the above-mentioned effects on the NLO properties, giving rise to compounds with  $\mu\beta$  values spanning from  $-2000 \times 10^{-48}$  esu to  $+3000 \times 10^{-48}$  esu.

## Experimental Section

**General Remarks.** Infrared spectra were measured by means of a Perkin-Elmer FTIR 1600 spectrometer (Nujol mulls) or a Bruker Equinox 55 FT-IR interferometer (KBr pellets). The Raman data were obtained using its FRA/106-S FT-Raman accessory kit. A continuous-wave Nd:YAG laser working at 1064 nm was employed for Raman excitation radiation with its power kept at a level lower than 100 mW. All the spectra were obtained with a spectral resolution of 4 cm<sup>-1</sup> and 50/3000 scans were averaged for each IR/Raman spectrum. Melting points were obtained on an Olympus BH-Z polarizing microscope equipped with a hot stage or in a Gallenkamp apparatus and are uncorrected. <sup>1</sup>H- and <sup>13</sup>C NMR spectra were recorded on a Bruker ARX300 or a Varian Unity-300 spectrometers operating at 300 and 75 MHz respectively;  $\delta$  values are given in ppm (relative to TMS) and  $J$  values in Hz. EI Mass spectra were recorded with a VG Autospec at

70 eV. Accurate mass measurements were obtained by narrow-range voltage scanning at 10 000 resolution (measured as peak width at 5% height) using perfluorokerosene as reference compound and were corrected to an accuracy of  $\pm 10$  ppm of the theoretical value. Electronic spectra were recorded with a UV-vis-NIR Cary 500 Scan spectrophotometer. Cyclic voltammetry measurements were performed with a  $\mu$ -Autolab ECO-Chemie potentiostat, using a glassy carbon working electrode, Pt counter electrode, and Ag/AgCl reference electrode. The experiments were carried out under argon, in  $\text{CH}_2\text{Cl}_2$  or DMF, with  $\text{Bu}_4\text{NPF}_6$  as supporting electrolyte (0.1 mol  $\text{L}^{-1}$ ). Scan rate was 100 mV  $\text{s}^{-1}$ .

**EFISH Measurements.** EFISH Measurements were taken with a nonlinear optics spectrometer from SOPRA. The fundamental light at 1.907  $\mu\text{m}$  was the first Stokes peak of a hydrogen Raman cell pumped by the 1.064  $\mu\text{m}$  light from a Q-switched Nd:YAG laser (Quantel YG 781, 10 pps, 8 ns, pulse). That light was passed through a linear polarizer and focused on the EFISH cell. The polarizing dc voltage (parallel to the light polarization) used in this cell was 6 kV. The output light from the cell was passed through an interference filter to select the second harmonic light (0.954  $\mu\text{m}$ ) which was finally detected with a R642 photomultiplier from Hamamatsu. Static  $\mu\beta(0)$  values were deduced from the experimental values using a two-level dispersion model.

**X-ray Single-Crystal Diffraction** data were collected at 294 K on a STOE-IPDS diffractometer equipped with a graphite monochromator utilizing MoK $\alpha$  radiation ( $\lambda = 0.71073$  Å). The structure was solved by direct methods using SIR92<sup>40</sup> and refined on  $F^2$  by full matrix least-squares techniques using SHELXL-97<sup>41</sup> with anisotropic thermal parameters for all non-hydrogen atoms. Absorption was corrected by multiscan technique and the H atoms were included in the calculation without refinement.

Crystal data for 5a: dark blue plate (0.63  $\times$  0.47  $\times$  0.08 mm<sup>3</sup>),  $\text{C}_{22}\text{H}_{26}\text{N}_2\text{S}_4$ , Mr = 446.69, triclinic, space group P-1,  $a = 7.4716(8)$  Å,  $b = 8.133(1)$  Å,  $c = 20.356(2)$  Å,  $\alpha = 97.94(1)^\circ$ ,  $\beta = 93.89(1)^\circ$ ,  $\gamma = 104.08(1)^\circ$ ,  $V = 1181.7(2)$  Å<sup>3</sup>,  $Z = 2$ ,  $\rho_{\text{calc}} = 1.255$  g cm<sup>-3</sup>,  $\mu$  (MoK $\alpha$ ) = 0.412 mm<sup>-1</sup>,  $F(000) = 472$ ,  $\theta_{\text{min}} = 2.03^\circ$ ,  $\theta_{\text{max}} = 25.76^\circ$ , 11517 reflections collected, 4196 unique ( $R_{\text{int}} = 0.0712$ ), restraints/parameters = 3/253,  $R_1 = 0.0546$  and  $wR_2 = 0.1298$  using 1630 reflections with  $I > 2\sigma(I)$ ,  $R_1 = 0.1379$  and  $wR_2 = 0.1587$  using all data, GOF = 0.821,  $-0.222 < \Delta\rho < 0.174$  e.Å<sup>-3</sup>.

**Computational Procedures.** All theoretical calculations were performed by using the Gaussian 03<sup>42</sup> program. The molecular geometries were optimized without symmetry restrictions unless otherwise stated using the B3P86<sup>43</sup> functional and the 6-31G(d)<sup>44</sup> basis set. The same model chemistry was used in TD-DFT calculations and the excited-state dipole moments were calculated by using the one particle RhoCI density. Molecular hyperpolarizabilities at zero frequency were calculated by the Coupled Perturbed Hartree-Fock Method (PCHF) using the HF/6-31G(d) model chemistry and the default parameters provided by the "polar" keyword. The default Gaussian 03 parameters were used in every case. Molecular orbital contours were plotted using Molekel 4.3.<sup>45</sup>

**2,6-Di-tert-butyl-4-([1,3]dithiol-2-ylidene)cyclohexa-2,5-dienone (2).** A solution of 2-methylsulfanyl-1,3-dithiolium iodide (1.035 g, 3.75 mmol) and 2,6-di-tert-butylphenol (2.317 g; 11.25 mmol) in 3.75 mL

of acetic acid and 0.56 mL of pyridine was refluxed under argon for 55 min. At the end of the reaction, the red solution was cooled to room temperature and water (100 mL) and  $\text{CH}_2\text{Cl}_2$  (100 mL) were added. The organic layer was separated and washed successively with 5% aqueous NaOH (2  $\times$  100 mL) and water (2  $\times$  100 mL). Then, it was dried over  $\text{MgSO}_4$ , evaporated and purified by column chromatography (silica gel) using  $\text{CH}_2\text{Cl}_2$  as eluent, giving an orange-red solid (260 mg, 23%); mp 199–202 °C (lit.<sup>46</sup> 192–195 °C);  $\delta_{\text{H}}$  ( $\text{CDCl}_3$ ) 7.02 (1H, s), 6.74 (1H, s), 1.30 (9H, s);  $\delta_{\text{C}}$  ( $\text{CDCl}_3$ ) 184.82, 160.39, 144.34, 126.54, 121.86, 117.72, 35.14, 29.47;  $\nu(\text{CO})$  1603  $\text{cm}^{-1}$ ; HRMS (EI): 306.1127 ( $\text{M}^+$ ) Calcd. for  $\text{C}_{17}\text{H}_{22}\text{OS}_2$  306.1112. Anal. Calcd. for  $\text{C}_{17}\text{H}_{22}\text{OS}_2$ : C, 66.62; H, 7.24; S, 20.92. Found: C, 66.76; H, 7.11; S, 20.80.

**2-[4-(4,5-Bis-pentylsulfanyl-[1,3]dithiol-2-ylidene)cyclohexa-2,5-dienylidene]-malononitrile (5a).** A solution of 2-methylsulfanyl-4,5-bis-pentylsulfanyl-[1,3]dithiolium tetrafluoroborate (316 mg, 0.72 mmol) and phenylmalononitrile (204 mg, 1.44 mmol) in a mixture of acetic acid (0.8 mL) and pyridine (0.08 mL) was refluxed under Ar for 45 min. After cooling, the blue mixture was filtered off and the resulting solid was washed with water, then with EtOH and then with Et<sub>2</sub>O to afford a first fraction (22 mg) of the desired compound. The filtrate was evaporated under vacuum and the resulting residue was dissolved in  $\text{CH}_2\text{Cl}_2$ ; the resulting solution was then successively washed with water, 5% aq. NaOH and water, dried with  $\text{Na}_2\text{SO}_4$  and evaporated under reduced pressure. Purification was effected by column chromatography on silica gel and elution with  $\text{CH}_2\text{Cl}_2$  gave 262 mg of a blue-violet solid (total yield 89%); mp 198–200 °C;  $\delta_{\text{H}}$  ( $\text{CDCl}_3$ ) 7.10 (1H, d,  $J = 9.1$  Hz), 7.03 (1H, d,  $J = 9.1$  Hz), 2.95 (2H, t,  $J = 7.4$  Hz), 1.68 (2H, q,  $J = 7.0$  Hz), 1.45–1.32 (4H, m), 0.92 (3H, t,  $J = 7.0$  Hz);  $\nu(\text{CN}^+)$  2195, 2166  $\text{cm}^{-1}$ ; HRMS (EI): 446.0983 ( $\text{M}^+$ ) Calcd. for  $\text{C}_{22}\text{H}_{26}\text{N}_2\text{S}_4$  446.0979. Anal. Calcd. for  $\text{C}_{22}\text{H}_{26}\text{N}_2\text{S}_4$ : C, 59.15; H, 5.87; N, 6.27; S, 28.71. Found: C, 59.32; H, 5.70; N, 6.43; S, 28.52.

**5-[4-(4,5-Bis-hexadecylsulfanyl-[1,3]dithiol-2-ylidene)cyclohexa-2,5-dienylidene]-1,3-dimethylpyrimidine-2,4,6-trione (7).** A solution of 4,5-bis-hexadecylsulfanyl-2-methylsulfanyl-[1,3]dithiolium tetrafluoroborate (262 mg, 0.35 mmol) and 1,3-dimethyl-5-phenylbarbituric acid (247 mg, 1.06 mmol) in a mixture of acetic acid (0.6 mL) and pyridine (0.1 mL) was refluxed under Ar for 45 min. After cooling to room temperature the resulting solid was filtered off, washed with water and then with EtOH and dried to afford the desired compound as a blue-violet solid: 256 mg, 86%; mp 59–60 °C;  $\nu(\text{CO})$  1678  $\text{cm}^{-1}$ ; MS (LSIMS): 845.5 ( $\text{M}+\text{H}^+$ ). Anal. Calcd. for  $\text{C}_{47}\text{H}_{76}\text{N}_2\text{O}_3\text{S}_4$ : C, 66.77; H, 9.06; N, 3.31; S, 15.17. Found: C, 66.90; H, 9.19; N, 3.46; S, 15.02.

**5-[4-(4,5-Bis-hexadecylsulfanyl-[1,3]dithiol-2-ylidene)cyclohexa-2,5-dienylidene]-1,3-diethyl-2-thioxodihydropyrimidine-4,6-dione (8).** This compound was prepared from 4,5-bis-hexadecylsulfanyl-2-methylsulfanyl-[1,3]dithiolium tetrafluoroborate (142 mg, 0.19 mmol) and 1,3-diethyl-5-phenylthiobarbituric acid (160 mg, 0.58 mmol) in a mixture of acetic acid (0.4 mL) and pyridine (0.056 mL), by using the same conditions as described above for 7. After cooling, the dark blue mixture was filtered and the solid was washed successively with water, EtOH and Et<sub>2</sub>O. The resulting solid was then treated with pentane to remove the unreacted 1,3-diethyl-5-phenylthiobarbituric acid, which was filtered off. After evaporation of pentane, the residue was purified by gradient column chromatography on silicagel ( $\text{CH}_2\text{Cl}_2$  followed by  $\text{CH}_2\text{Cl}_2/\text{EtOAc}$  97:3), to afford a deep blue solid: 131 mg, 77%; mp 57 °C;  $\delta_{\text{H}}$  ( $\text{CDCl}_3$ ) 8.83 (1H, d,  $J = 9.1$  Hz), 7.45 (1H, d,  $J = 9.1$  Hz), 4.65 (2H, q,  $J = 7.0$  Hz), 3.05 (2H, t,  $J = 7.3$  Hz), 1.25 (31H, s), 0.88 (3H, t,  $J = 7.0$  Hz);  $\nu(\text{CS})$  1106  $\text{cm}^{-1}$ ; MS (LSIMS): 888.5 ( $\text{M}^+$ ). Anal. Calcd. for  $\text{C}_{49}\text{H}_{80}\text{N}_2\text{O}_3\text{S}_5$ : C, 66.16; H, 9.07; N, 3.15; S, 18.02. Found: C, 66.01; H, 9.22; N, 3.31; S, 17.83.

**2-[4-(2-[1,3]Dithiol-2-ylidenethylidene)cyclohexa-2,5-dienylidene]-malononitrile (10a).** To a solution of [1,3]dithiol-2-ylideneacetaldehyde (44 mg, 0.305 mmol) in acetic anhydride (1 mL), phenylmalononitrile

(40) SIR92 – A program for crystal structure solution. Altomare, A.; Cascarano, G.; Giacovazzo, C.; Guagliardi, A. *J. Appl. Crystallogr.* **1993**, *26*, 343–350.

(41) SHELX97 [Includes SHELXS97, SHELXL97, CIFTAB (and SHELXA)] – Programs for Crystal Structure Analysis (Release 97–2). Sheldrick, G. M., Institut für Anorganische Chemie der Universität, Tammanstrasse 4, D-3400 Göttingen, Germany, 1998.

(42) Gaussian 03, Revision B.05, Frisch, M. J. et al.; Gaussian, Inc., Pittsburgh, PA, 2003.

(43) The B3P86 Functional consists of Becke's three parameter hybrid functional (Becke, A. D. *J. Chem. Phys.* **1993**, *98*, 5648–5652) with the nonlocal correlation provided by the Perdew 86 expression: Perdew, J. P. *Phys. Rev. B* **1986**, *33*, 8822–8824.

(44) Hariharan, P. C.; Pople, J. A. *Theor. Chim. Acta* **1973**, *28*, 213–222.

(45) Portmann, S.; Lüthi, H. P. *Chimia* **2000**, *54*, 766–770.

(46) Schaumann, E.; Winter-Extra, S.; Kummert, K.; Scheiblich, S. *Synthesis* **1990**, 271–273.

(43.3 mg, 0.305 mmol) was added and the mixture was heated at 75–80 °C under Ar for 20–30 min. After cooling to room temperature the resulting solid was filtered off, washed successively with water, cold EtOH and Et<sub>2</sub>O and dried to afford the desired compound as a dark green solid: 12 mg, 15%; mp > 300 °C;  $\nu(\text{CN})$  2190, 2159 cm<sup>-1</sup>; MS (EI): 268 (M<sup>+</sup>). Anal. Calcd. for C<sub>14</sub>H<sub>8</sub>N<sub>2</sub>S<sub>2</sub>: C, 62.66; H, 3.00; N, 10.44; S, 23.90. Found: C, 62.83; H, 3.13; N, 10.59; S, 23.72.

**2-[4-(2-(4,5-Ethylenedisulfanyl-[1,3]dithiol-2-ylideneethylidene))-cyclohexa-2,5-dienylidene]malononitrile (10b).** To a solution of 4,5-ethylenedisulfanyl[1,3]dithiol-2-ylideneacetaldehyde (117 mg, 0.5 mmol) in acetic anhydride (3 mL), phenylmalononitrile (81 mg, 0.57 mmol) was added and the mixture was refluxed under Ar for 5 h. After cooling and evaporation of the solvent under vacuum, the residue was purified by column chromatography (silica gel) using CH<sub>2</sub>Cl<sub>2</sub> as eluent, giving a dark-blue solid (35 mg, 20%); mp 238–241 °C (d); due to its low solubility its <sup>1</sup>H NMR spectrum could not be registered;  $\nu(\text{CN})$  2189, 2157 cm<sup>-1</sup>; HRMS (EI): 357.9726 (M<sup>+</sup>) Calcd. for C<sub>16</sub>H<sub>10</sub>N<sub>2</sub>S<sub>4</sub> 357.9727. Anal. Calcd. for C<sub>16</sub>H<sub>10</sub>N<sub>2</sub>S<sub>4</sub>: C, 53.60; H, 2.81; N, 7.81; S, 35.77. Found: C, 53.49; H, 2.99; N, 7.68; S, 35.90.

**2-[4-(2-[1,3]Dithiol-2-ylideneethylidene)-4H-naphthalen-1-ylidene]-malononitrile (11a).** To a solution of [1,3]dithiol-2-ylideneacetaldehyde (40 mg, 0.277 mmol) in acetic anhydride (2 mL), 1-naphthylmalononitrile (53.3 mg, 0.277 mmol) was added and the mixture was heated at 75–80 °C under Ar for 60 min. By using the same workup and purification procedure as described for **10a**, a green solid was obtained: 42 mg, 48%; mp darkening from ca. 250 °C;  $\delta_{\text{H}}$  (DMSO-*d*<sub>6</sub>) 8.85 (1H, dd, *J* = 1.2, 8.5 Hz), 8.45 (1H, d, *J* = 8.5 Hz), 8.16 (1H, d, *J* = 13.5 Hz), 8.12 (1H, d, *J* = 9.7 Hz), 7.86 (1H, d, *J* = 13.5 Hz), 7.72 (1H, ddd, *J* = 1.2, 8.5, 8.5 Hz), 7.64 (s, 2H), 7.55 (1H, ddd, *J* = 1.2, 8.5, 8.5 Hz), 7.20 (1H, dd, *J* = 1.2, 9.7 Hz);  $\nu(\text{CN})$  2194, 2180 cm<sup>-1</sup>; HRMS (EI): 318.0297 (M<sup>+</sup>) Calcd. for C<sub>18</sub>H<sub>10</sub>N<sub>2</sub>S<sub>2</sub> 318.0285. Anal. Calcd. for C<sub>18</sub>H<sub>10</sub>N<sub>2</sub>S<sub>2</sub>: C, 67.90; H, 3.17; N, 8.80; S, 20.14. Found: C, 67.74; H, 3.33; N, 8.62; S, 20.31.

**2-[4-(2-(4,5-Ethylenedisulfanyl-[1,3]dithiol-2-ylideneethylidene))-4H-naphthalen-1-ylidene]malononitrile (11b).** To a solution of 4,5-ethylenedisulfanyl[1,3]dithiol-2-ylideneacetaldehyde (117 mg, 0.5 mmol)

in acetic anhydride (4 mL), 1-naphthylmalononitrile (110 mg, 0.57 mmol) was added and the mixture was heated at 75 °C under Ar for 5 h. After cooling at room temperature and then at 4 °C, the mixture was filtered off and the resulting green solid was washed with water and then with EtOH to afford a first fraction (56 mg) of the desired compound. To the filtrate CH<sub>2</sub>Cl<sub>2</sub> (50 mL) was added and the resulting solution was then successively washed with water, 1M aq. NaHCO<sub>3</sub> and water, dried with MgSO<sub>4</sub> and evaporated under vacuum. Column chromatography (silica gel) of the residue using CH<sub>2</sub>Cl<sub>2</sub> as eluent afforded a second fraction (53 mg) of the final product. In all, 109 mg (53%) of a green solid were obtained; mp 232–236 °C; due to its low solubility its <sup>1</sup>H NMR spectrum could not be registered;  $\nu(\text{CN})$  2195, 2178 cm<sup>-1</sup>; HRMS (EI): 407.9873 (M<sup>+</sup>) Calcd. for C<sub>20</sub>H<sub>12</sub>N<sub>2</sub>S<sub>4</sub> 407.9883. Anal. Calcd. for C<sub>20</sub>H<sub>12</sub>N<sub>2</sub>S<sub>4</sub>: C, 58.79; H, 2.96; N, 6.86; S, 31.39. Found: C, 58.62; H, 2.76; N, 6.98; S, 31.54.

**Acknowledgment.** J.C. is grateful to the Ministerio de Ciencia y Tecnología (MCyT) of Spain for a Ramón y Cajal research position of Chemistry at the University of Málaga. We thank MCyT-FEDER (BQU2002-00219, BQU2003-03194) for financial support. We are grateful to Dr. Nazario Martín for samples of compounds **12c**, **12d**, **13c** and **13d**. M.C.R.D. acknowledges the MEC for a personal grant. L. C. acknowledges MEC for a FPU grant.

**Supporting Information Available:** Complete refs 8, 20b, 22a, 22b, and 42. Cartesian coordinates of optimized geometries used in theoretical calculations. Crystallographic data, tables of bond distances and angles, positional parameters, and general displacement parameters for **5a**. Selected B3P86/6-31G(d) Raman-active vibrational eigenvectors for **5c**, **10a** and **11a**. X-ray crystallographic file in CIF format with the coordinates of molecule **5a**. This material is available free of charge via the Internet at <http://pubs.acs.org>.

JA051819L